Effect of phospholipids on the structure of *Triatoma infestans* lipophorin studied by fluorescence methods

Omar J. Rimoldi,[1] Horacio A. Garda, and Rodolfo R. Brenner

Instituto de Investigaciones Bioquímicas de la Plata (INIBIOLP), CONICET-UNLP, Facultad de Ciencias Médicas, 60 y 120, 1900-La Plata, Argentina

Abstract To study the role of phospholipids in the lipophorin structure, they were removed by phospholipase A_2 treatment. Fluorescence lifetimes and accessibility to acrylamide quenching of different diphenylhexatrienyl derivatives, which were used as analogues of the different lipid components, indicate a surface localization of phospholipids and a distribution of diacylglycerols between the core and the surface, the surface fraction being increased by the phospholipase A_2 treatment. The rotational behavior of these probes, studied by differential polarized phase fluorescence, indicates a high lipid order not only in the surface layer where phospholipids are located, but also in the core occupied by diacylglycerols and hydrocarbons. Phospholipid depletion increases the order only in the external region of the surface layer. Energy transfer from apolipoprotein tryptophan residues to several fluorescent acceptors indicates that phospholipid depletion produces a re-accommodation of the apoproteins. A decreased mobility of the water in the interfacial region is also produced by the phospholipase A_2 treatment as it is reported by the fluorescence of 6-lauroyl-2-dimethylaminonaphthalene. This work shows that phospholipase A_2 treatment of *T. infestans* lipophorin results in stable particles with an increased diacylglycerol to phospholipid ratio in the surface lipid layer. The modified particles are possibly stabilized by a conformational change in the apolipoproteins.—**Rimoldi, O. J., H. A. Garda, and R. R. Brenner.** Effect of phospholipids on the structure of *Triatoma infestans* lipophorin studied by fluorescence methods. *J. Lipid Res.* 1996. **37:** 2125–2135.

Supplementary key words *Triatoma infestans* • lipophorin • phospholipase A_2 fluorescence quenching • energy transfer • Laurdan generalized polarization • differential polarized phase fluorescence • insect

Insects primarily use a single type of lipoprotein, lipophorin (Lp), for the transport of phospholipids (PL), diacylglycerols (DAG), hydrocarbons (HC), sterols and free fatty acids (1–3). A challenging problem to understand lipid transport in insects is the elucidation of Lp structure and organization of its proteins and lipid components. HC seem to be located in the interior of the particle unexposed to water environment (4). The localization of DAG in the Lp particle is still under discussion (3, 5). A composition–structure correlation model for Lp without apoLp III seems to be consistent with the majority of DAG molecules located in the hydrophobic lipid core (6). The PL content is linearly related to the Lp size (6) and it has been determined that PL are located on the Lp surface (7).

Another question is how large variations in lipid content and composition can be accommodated without modification in the apolipoprotein composition of the Lp particles. Enzymatic depletion of PL has been used to alter the Lp structure and lipid composition. Phospholipase A_2 (PLA_2) digestion of *M. sexta* (8) and *R. prolixus* Lp (9) resulted in stable PL-depleted particles. In other studies, four subspecies of Lp with different amounts of DAG showed aggregation and particle fusion after digestion with phospholipase C (10).

In this work, the effect of PL depletion by PLA_2 digestion on the structure and organization of the protein and lipid components of *T. infestans* Lp was studied. 2-(3-(Diphenyl-hexatrienyl)propanoyl)-3-palmitoyl-L-α-phosphatidylcholine (DPH-PC) and 2-(3-(diphenyl-hexatrienyl)propanoyl)-3-palmitoyl-L-α-glycerol (DPH-DAG) were used as fluorescent analogues of PL and DAG, respectively. Lifetimes (τ) and accessibility to acrylamide of these probes were measured to obtain information on the localization of PL and DAG in the Lp particles

Abbreviations: apoLp, apolipophorin; n-AS, n-(9-anthroyloxy)stearate; DAG, diacylglycerol; DPH, 1,6-diphenyl-1,3,5-hexatriene; DPH-DAG, 2-(3-(diphenylhexatrienyl)propanoyl)-3-palmitoyl-L-α-glycerol; DPH-PC, 2-(3-(diphenylhexatrienyl)propanoyl)-3-palmitoyl-L-α-phosphatidylcholine; DPH-Prop, 3-(p-(6-phenyl)-1,3,5-hexatrienyl)phenylpropionate; DPH-TMA, 1-(4-trimethylammoniumphenyl)-6-phenyl-1,3,5-hexatriene; GP, generalized polarization; HC, hydrocarbons; Laurdan, 6-lauroyl-2-dimethylaminonaphthalene; Lp, lipophorin; PL, phospholipids; PLA_2, phospholipase A_2; rs, steady-state fluorescence anisotropy; r_∞, limiting anisotropy; Trp, tryptophan; τ, fluorescence lifetime; τ_M, τ obtained from the demodulation ratio; τ_P, τ obtained from the phase shift; $\langle\tau\rangle$, average between τ_M and τ_P; τ_R, rotational correlation time.

[1]To whom correspondence should be addressed.

and their redistribution after PLA_2 treatment. Other probes such as 1,6-diphenyl-1,3,5-hexatriene (DPH) whose hydrophobicity allows us to predict a similar localization as HC, or 3-(p-(6-phenyl)-1,3,5-hexatrienyl)phenylpropionate (DPH-Prop) and 1-(4-trimethyl-ammoniumphenyl)-6-phenyl-1,3,5-hexatriene (DPH-TMA) which are anchored to the interface through their charged groups, were used for comparison. Differential polarized phase fluorescence was used to study the rotational behavior of these probes to obtain information on the order and dynamics of the different regions of Lp as well as the effect of PLA_2 treatment (11, 12). Acrylamide quenching of apoprotein tryptophan (Trp) fluorescence and energy transfer from Trp to DPH, DPH-Prop and a set of n-(9-anthroyloxy)stearates (n-AS) (where n = 2, 7, and 12) were also used to provide information on the relative localization of apoprotein Trp residues (13). In addition, we have used 6-lauroyl-2-dimethylaminonaphthalene (Laurdan), a probe sensible to the mobility of the water in the polar group region in order to sense the changes in the interfacial properties (14, 15).

MATERIALS AND METHODS

Materials

PLA_2 from *Crotalus durisis* was purchased from Sigma Chemical Company (St. Louis, MO). DPH was obtained from Aldrich Company (Milwaukee, WI). DPH-TMA, DPH-Prop, DPH-PC, 2,7, and 12-AS and Laurdan were purchased from Molecular Probes Inc. (Junction City, OR). DPH-DAG was obtained by digestion of DPH-PC liposomes (1 mg/ml) with 5 units of phospholipase C from *Bacilus cereus* (Sigma Chemical Co., St. Louis, MO) at 37°C for 3 h, under N_2. DPH-DAG was then isolated by TLC as described below for lipid analysis.

Lipophorin isolation

T. infestans Lp was isolated from hemolymph by density gradient ultracentrifugation as described by Rimoldi et al. (16) and purified by gel filtration HPLC using an Ultro Pac TSK-G 3000 SW (300 × 7.5 mm ID) columm equilibrated and eluted with 0.05 M Tris-HCl buffer, pH 7.5, and 0.15 M NaCl. Lp peak was concentrated with Centripep-30 (Amicon Corp.) and its protein content was determined by the method of Lowry et al. (17) using bovine serum albumin as standard.

Treatment of lipophorin with phospholipase A_2

The purified Lp was incubated at 37°C for 3 h in a reaction medium containing fatty acid-free albumin (25 mg albumin/mg Lp). PLA_2 (5 U/mg Lp) was added to 0.5 M NaCl, 0.02 M sodium azide, and 3 mM $CaCl_2$ in 50 mM Tris-HCl buffer, pH 7.5. As control, Lp was incubated in a reaction medium containing albumin but lacking PLA_2. Treated Lp was separated from albumin by HPLC as described above. The Lp fraction was examined by native PAGE (18).

Lipid analysis

The Lp total lipids were extracted with chloroform–methanol (19). Lipid classes were separated by TLC on silica gel-G with hexane–diethylether–acetic acid 80:20:1 (v/v). To quantitate DAG and PL, internal standards of 1,2 dieicosenoylglycerol and 1,2 dieicosenoyl-*sn*-glycero-3-phosphocholine were added to the Lp prior to the extraction. After separating the lipids by TLC, the fractions of DAG and PL were scraped off the plate and eluted with chloroform–methanol–hexane 2:1:3 (v:v:v). The solvent was evaporated under N_2 and the samples were *trans*-esterified by heating at 64°C for 3 h in 14% boron trifluoride in methanol. The resulting methyl esters were separated on a column of SP 2330 on 100–200 mesh Chromosorb WAW using a Hewlett-Packard 5840 A gas–liquid chromatograph.

Fluorescence studies

All the measurements were made at 25°C in an SLM 4800 C spectrofluorometer (SLM Instruments, Inc., Urbana, IL). Lp was labeled by incubation with the corresponding probes at room temperature and darkness. Unless otherwise indicated, the probe/lipid molar ratio was about 1:200. Labeling with DG-DPH and PC-DPH required 12 h of incubation. For the other probes 30 min were required.

Lifetime determinations

Lifetimes were measured by excitation with amplitude modulated light at 18 and 30 MHz through a Debye-Sears modulator, and by measuring the phase shift and demodulation ratio with respect to a solution of a reference compound (20). Excitation with vertically polarized light and observation of the emission through a polarizer at 55° were used to eliminate the effect of the sample polarization on the τ measurements (21). The reference solutions were POPOP (1,4-bis(5-phenyloxazol-2-yl)benzene) in ethanol (τ = 1.35 ns) (22, 23) to measure the τ of DPH-derivatives, Laurdan and n-AS, or p-terphenilo (τ = 1.05 ns) (11, 24) to measure the τ of Trp. Excitation wavelength was 361 nm for DPH-derivatives and n-AS, 360 nm for Laurdan and 290 nm for Trp. Emission was observed through a sharp cut-off filter KV 389 for DPH-derivatives, KV 418 for Laurdan, KV 408 for n-AS, and at different emission wavelengths using monochromator bandpass of 8 nm for Trp.

Steady-state and dynamic polarization measurements

To estimate the rate and range of the wobbling rotation of DPH-derivatives in Lp, the rotational correlation time (τ_R) and the limiting anisotropy (r_∞) were calculated from measurements of steady-state anisotropy (r_S), τ, and the differential polarized phase shift (Δ) according to Weber theory (25); Δ was determined according to Lakowicz (11) and Lakowicz, Prendergast, and Hogen (12) as previously described (26, 27). Fundamental anisotropy (r_O) used in the calculations for τ_R and r_∞ was 0.390 as previously estimated (28).

Acrylamide quenching measurements

Fo/F ratios were plotted versus acrylamide concentration, where Fo and F were the fluorescence intensities in the absence and in the presence of acrylamide, respectively. They were obtained by exciting at 361 nm and integrating the emission spectra between 380 and 598 nm for the DPH derivatives, and by exciting at 290 and integrating the emission spectra between 300 and 395 nm for Trp.

Energy transfer

Energy transfer from Trp to DPH, DPH-Prop, and n-AS was measured by exciting at 290 nm and integrating the emission spectra between 300 and 380 nm. Energy transfer efficiency (1 - Fo/F) was plotted versus the acceptor/lipid molar ratio. Only PL and DAG were considered to calculate the acceptor/lipid molar ratio.

Laurdan generalized polarization (GP)

Native and PLA_2-treated Lp (60 μg of protein/ml) were labeled with 1 μM Laurdan. Emission spectra were taken at different excitation wavelengths using monochromator bandpasses of 8 nm for excitation and 4 nm for emission. Excitation spectra were taken at different emission wavelengths using bandpasses of 4 nm for excitation and 8 nm for emission.

Excitation generalized polarization (ex GP) values were calculated at different excitation wavelengths from (29):

$$\text{ex GP} = (I_{435} - I_{490})/(I_{435} + I_{490})$$

where I_{435} and I_{490} were the intensities at each excitation wavelength, obtained using fixed emission wavelength of 435 and 490 nm, respectively. The emission GP (em GP) values were calculated at different emission wavelengths from:

$$\text{em GP} = (I_{410} - I_{340})/(I_{410} + I_{340})$$

where I_{410} and I_{340} were the intensities at each emission wavelength, obtained using fixed excitation wavelengths of 410 and 340 nm, respectively.

RESULTS

Phospholipase A_2 treatment of lipophorin

The PL/DAG molar ratio was 0.67 in native Lp and it decreased to 0.17 in PLA_2-treated Lp. TLC analysis indicated that after treatment the lysophospholipids and free fatty acids formed were associated to albumin but not to Lp. Treatment increased buoyant density of Lp from 1.115 to 1.132 as it was detected by centrifugation in a NaBr gradient (**Fig. 1A**). PL depletion also resulted in smaller particles (Fig. 1B).

Fluorescence lifetimes and rotational behavior of DPH-derivatives

Phase (τ_P) and modulation (τ_M) lifetimes obtained at 18 MHz of excitation frequency for DPH-derivatives incorporated in native and PLA_2-treated Lp, are shown in **Table 1.** Heterogeneity in τ is indicated by the discrepancies between τ_P and τ_M and also by the lower τ obtained at 30 MHz excitation (not shown). Heterogeneity in τ can be due not only to several fluorophore populations with different transversal or lateral localizations, but also to a population with a broad τ distribution (30). Despite the difficulties in resolving this heterogeneity from measurements at two excitation frequencies, the average of τ_P and τ_M ($\langle\tau\rangle$) indicates that water content and/or polarity of the probe environment decrease in the order DPH-TMA > DPH-Prop > DPH-PC > DPH-DAG > DPH in both native and PLA_2-treated Lp.

The large $\langle\tau\rangle$ of DPH indicates that it is located in a environment of very low polarity, possibly the hydrophobic Lp core. On the contrary, shorter $\langle\tau\rangle$ are observed for the anphipatic DPH-TMA, DPH-Prop, and DPH-PC, which are anchored to the interface of the Lp particle through their charged groups. From the chemical structure and $\langle\tau\rangle$ of DPH-TMA, DPH-Prop, and DPH-PC, it is possible to predict that although all these probes would be located in the surface layer of the Lp particle, the depth of the fluorescent moiety localization would be in the order DPH-PC > DPH-Prop > DPH-TMA.

The $\langle\tau\rangle$ obtained for DPH-DAG suggests that the environment of this probe has an intermediate polarity between DPH and DPH-PC environments. However, a distribution of DPH-DAG between a pool similar to DPH and another one similar to the surface probes is also possible. The greatest discrepancy between τ_P and τ_M for DPH-DAG in comparison with the other probes

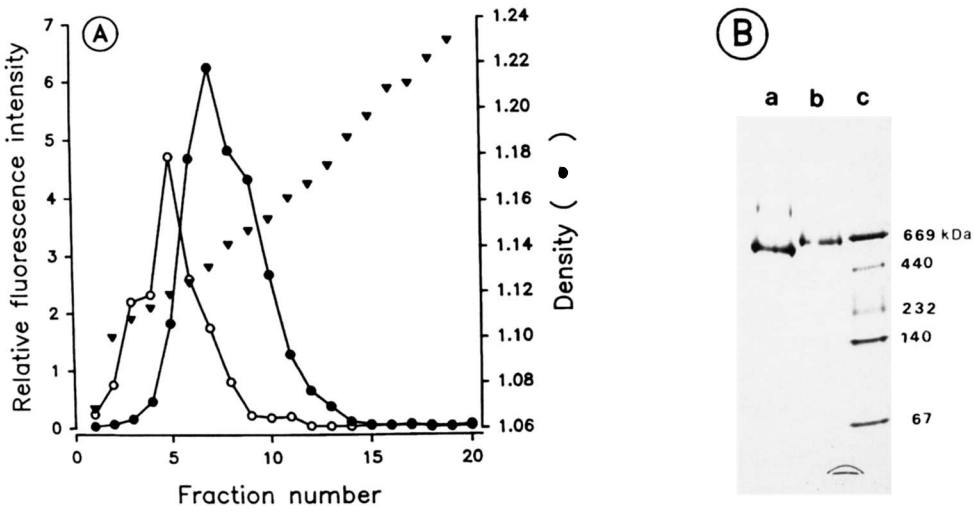

Fig. 1. A: Density-gradient ultracentrifugation of native (open symbols) and phospholipase A_2-treated lipophorin (filled symbols). The proteins were monitored in the fractions by tryptophan fluorescence intensity and the densities were determined by measuring the refractive index of NaBr at 26°C (triangles). B: Native polyacrylamide gel electrophoresis of phospholipase A_2-treated lipophorin (line a) and native lipophorin (line b). A 4–20% polyacrylamide gradient slab gel was used. Molecular weight standards (line c): thyroglobulin (M_r 669 kDa), ferritin (440 kDa), catalase (232 kDa), lactate dehydrogenase (140 kDa), and albumin (67 kDa).

indicates a more heterogeneous τ distribution which seems to support the last possibility.

While <τ> values for DPH, DPH-Prop, and DPH-PC are not changed, a small but significant decrease in <τ> of DPH-TMA is produced by PLA_2 treatment. This can be due to an increased water penetration in the more external region of the surface layer resulting from PL depletion. On the other hand, <τ> of DPH-DAG is largely shortened, indicating a particularly large polarity increase in the average environment of this DAG analogue after PLA_2 treatment. This indicates a specific effect of PL depletion on the environment of DPH-DAG or, what is more probable, a redistribution of DPH-DAG. The surface-located fraction of DPH-DAG would be increased at the expense of the core fraction. The increase observed in the differences between τ_P and τ_M indicates an increased τ heterogeneity which would support this possibility.

Although the τ heterogeneity does not allow the exact calculation of the rotational parameters from the differential polarized phase data, average rotational correlation time (τ_R) and limiting anisotropy (r_∞) values can be calculated using <τ> (31). They are shown in Table 1. From the r_∞ values it can be concluded that the surface-located probes (DPH-PC, DPH-Prop, and DPH-TMA) wobble with less amplitude in comparison with the

TABLE 1. Fluorescence lifetimes and rotational behavior of DPH-derivative probes in native and phospholipase A_2-treated lipophorin of *T. infestans*

Probe	Sample	τ_P	τ_M	<τ>	r_S	τ_R	r_∞
DPH	N-Lp	8.4 ± 0.1	9.0 ± 0.1	8.7	0.220 ± 0.002	2.8 ± 0.3	0.16 ± 0.01
DPH	T-Lp	8.2 ± 0.1	9.1 ± 0.1	8.6	0.230 ± 0.002	2.8 ± 0.3	0.18 ± 0.01
DPH-DAG	N-Lp	6.4 ± 0.1	7.5 ± 0.2	6.9	0.257 ± 0.003	3.6 ± 0.4	0.18 ± 0.02
DPH-DAG	T-Lp	5.1 ± 0.1	6.8 ± 0.1	5.9	0.253 ± 0.003	3.6 ± 0.4	0.17 ± 0.02
DPH-PC	N-Lp	5.9 ± 0.1	6.7 ± 0.2	6.3	0.279 ± 0.005	2.2 ± 0.5	0.24 ± 0.03
DPH-PC	T-Lp	6.0 ± 0.1	6.8 ± 0.2	6.4	0.281 ± 0.004	2.7 ± 0.4	0.23 ± 0.02
DPH-Prop	N-Lp	5.7 ± 0.1	6.2 ± 0.1	5.9	0.303 ± 0.002	3.1 ± 0.3	0.26 ± 0.02
DPH-Prop	T-Lp	5.5 ± 0.1	5.8 ± 0.1	5.7	0.312 ± 0.002	1.7 ± 0.2	0.29 ± 0.02
DPH-TMA	N-Lp	4.4 ± 0.1	5.0 ± 0.1	4.7	0.292 ± 0.002	2.5 ± 0.3	0.24 ± 0.02
DPH-TMA	T-Lp	3.7 ± 0.1	4.5 ± 0.1	4.1	0.320 ± 0.003	0.9 ± 0.2	0.30 ± 0.02

The means of six measurements and standard deviations are given. Lifetimes and rotational correlation times are in nanoseconds. N-Lp is native lipophorin and T-Lp is phospholipase A_2-treated lipophorin.

deeply located DPH, which suggests a higher ordering in the surface lipid layer as compared with the lipid core. PLA_2 treatment does not seem to affect the rotational behavior of DPH, DPH-DAG, and DPH-PC. However, calculated τ_R and r_∞ values indicate that DPH-Prop and specially DPH-TMA wobble faster but in a more restricted range in PL depleted than in native Lp. Thus, PLA_2 treatment seems to increase the ordering only in the external region of the surface layer, mainly sensed by DPH-TMA and in a minor degree by DPH-Prop but not by DPH-PC.

The r_S is higher for DPH-DAG than for DPH in both native and PL-depleted Lp. This is due to a slow rotational rate as it is indicated by τ_R, but no differences are apparent in r_∞ values indicating a similar ordering in the environments of these probes. This fact together with no effect of PL depletion on the DPH-DAG rotational behavior do not apparently support the possibility of a distribution of DPH-DAG between a core and a surface pool. However, it is worth noting that for such distribution the core fraction would be preferentially weighed, due to its higher τ and quantum yield in comparison with the surface pool. Thus, for a low proportion of DPH-DAG in the surface fraction, the expected increase in r_∞ is not larger than the experimental errors of these measurements.

Acrylamide quenching of DPH-derivative probes

Stern-Volmer plots for acrylamide quenching of DPH-derivatives incorporated in native and PLA_2-treated Lp are shown in **Fig. 2.** Upward deviations, usually attributed to mixed quenching mechanisms, are evident for the highly quenched probes such as DPH-TMA, DPH-Prop, and DPH-PC. The possibility of mixed static and dynamic quenching was investigated by measuring the effect of quencher on τ. Acrylamide has a lesser effect on τ (**Table 2**) than on fluorescence intensity (Fig. 2), suggesting a high proportion of static quenching. However, it must be noted that heterogeneous fluorophore populations can also result in a low influence on τ. As acrylamide will quench preferentially the more exposed fluorophore populations with shorter τ, leaving unquenched the populations with larger τ, it may result in smaller effects and even in apparent increases in the average τ.

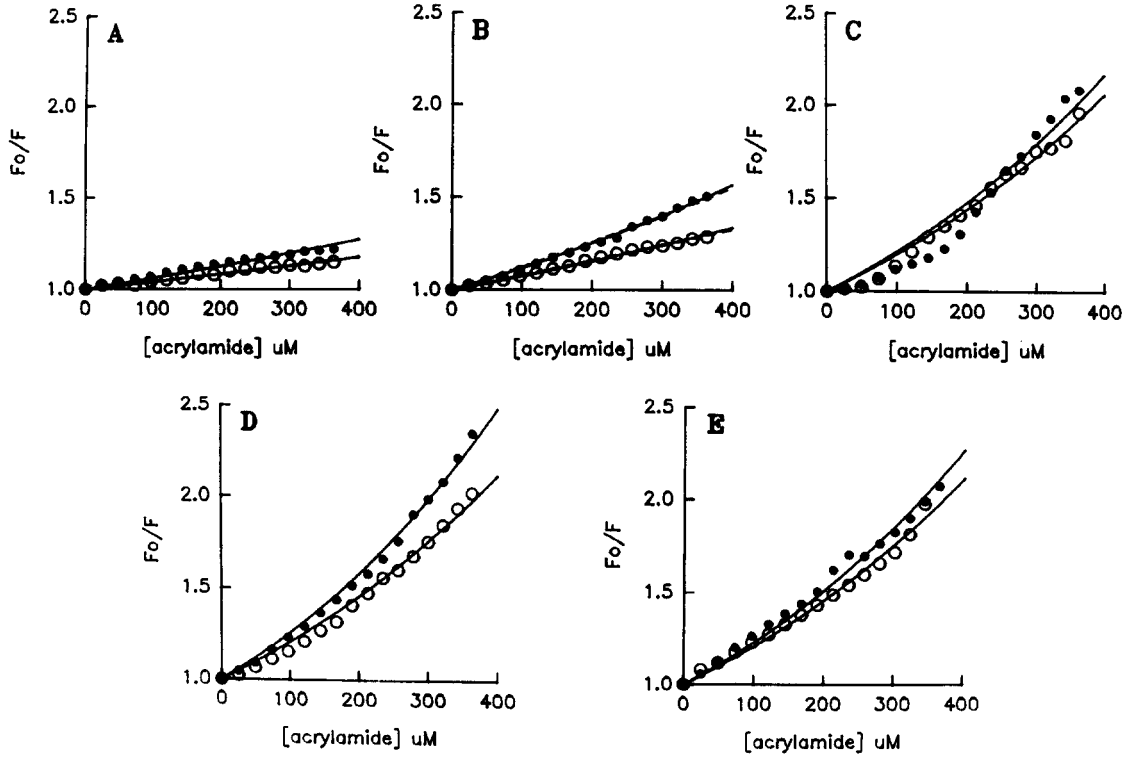

Fig. 2. Stern-Volmer plots for acrylamide quenching of the fluorescence of DPH (A), DPH-DAG (B), DPH-PC (C), DPH-Prop (D), and DPH-TMA (E) incorporated in native (open symbols) and phospholipase A_2-treated (filled symbols) lipophorin. The best fit to the data using the equation: $Fo/F = (1 + K\,Q)\exp(\alpha\,K\,Q)$ assuming $\alpha = 5$ are shown (—). In B, the simulated curves using the equation: $Fo/F = (f/[Fo/F]_1 + (1 - f)/[Fo/F]_2)^{-1}$, are also shown; where $[Fo/F]_1$ and $[Fo/F]_2$ are the best fits to the data of DPH and DPH-PC shown in A and C, respectively, and the fractional intensity f is 0.75 and 0.55 for native and treated lipophorin, respectively. These curves are undistinguishable from those when a unique population is assumed.

TABLE 2. Acrylamide quenching of DPH-derivatives in native and phospholipase A_2-treated lipophorin of *T. infestans*

Probe	Sample[a]	τ_O/τ[b]	K (M^{-1})[c] α = 2	α = 5	α = 10
DPH	N-Lp	1.06	0.136 ± 0.003 (1.00)	0.068 ± 0.002 (1.00)	0.037 ± 0.001 (1.00)
DPH	T-Lp	1.07	0.202 ± 0.005 (1.48)	0.100 ± 0.002 (1.48)	0.055 ± 0.001 (1.48)
DPH-DAG	N-Lp	0.97	0.244 ± 0.002 (1.79)	0.121 ± 0.001 (1.78)	0.066 ± 0.001 (1.78)
DPH-DAG	T-Lp	0.96	0.380 ± 0.003 (2.78)	0.188 ± 0.001 (2.76)	0.102 ± 0.001 (2.76)
DPH-PC	N-Lp	1.06	0.622 ± 0.009 (4.56)	0.305 ± 0.(4.49)004 (4.49)	0.165 ± 0.002 (4.47)
DPH-PC	T-Lp	1.09	0.667 ± 0.021 (4.88)	0.326 ± 0.010 (4.81)	0.177 ± 0.005 (4.79)
DPH-Prop	N-Lp	1.07	0.644 ± 0.008 (4.72)	0.315 ± 0.004 (4.64)	0.171 ± 0.002 (4.62)
DPH-Prop	T-Lp	1.05	0.786 ± 0.007 (5.76)	0.383 ± 0.003 (5.64)	0.208 ± 0.002 (5.61)
DPH-TMA	N-Lp	1.03	0.644 ± 0.008 (4.72)	0.316 ± 0.004 (4.65)	0.171 ± 0.002 (4.63)
DPH-TMA	T-Lp	1.04	0.708 ± 0.008 (5.18)	0.346 ± 0.004 (5.09)	0.187 ± 0.002 (5.06)

[a]N-Lp, native lipophorin; T-Lp, phospholipase A_2-treated lipophorin.
[b]τ_O and τ are the lifetimes (average of τ_P and τ_M) in the absence and in the presence of 0.4 M acrylamide, respectively.
[c]Quenching constants and standard errors obtained by fitting the equation: $Fo/F = (1 + K\,Q)\exp(\alpha\,K\,Q)$ to the experimental data in Fig. 2. Different values of α were assumed. In parentheses, the values of K relative to that for DPH in native lipophorin are shown.

The impossibility of resolving the heterogeneity in fluorophore populations precludes the exact quantitation of the individual contributions of static and dynamic quenching. However, as both quenching mechanisms depend on the fluorophore accessibility to the quencher, a simple treatment was used to quantitate an average accessibility of these probes to acrylamide. Experimental data were fitted to the equation $Fo/F = (1 + K\,Q)\exp(V\,Q)$ (32), where K is the dynamic and V the static quenching constants, and Q is the quencher concentration. A constant ratio between K and V ($\alpha = V/K$) was assumed for all the DPH-derivatives, as it was expected for the same quencher and fluorescent moiety (32). The best fittings were obtained with α values between 2 and 10. These high values for α indicate a high proportion of static quenching in concordance with the low influence on τ. Although there exists a large uncertainty about α and thus about the absolute dynamic and static quenching constants, Table 2 shows that the relative changes in the values obtained for K in the different probes and samples are practically independent of the value selected for α. Thus, the relative values of K indicate relative accessibility to acrylamide.

Accessibility to acrylamide in both native and PLA_2-treated Lp was in the order DPH < DPH-DAG < DPH-PC ≈ DPH-Prop ≈ DPH-TMA. This is in good concordance with the environment polarity and/or water accessibility indicated by <τ> values.

The relative unaccessibility of DPH to acrylamide indicates that this probe is far from the aqueous medium. On the contrary, acrylamide accesses to the PL analogue DPH-PC as easily as to DPH-Prop and DPH-TMA, which are anchored to the interface, suggesting that PL are superficially located in the Lp particles.

On the other hand, the DAG analogue DPH-DAG has an intermediate accessibility to acrylamide, suggesting a localization for DAG intermediate between HC and PL or, as above mentioned, a distribution between a core and a surface localization. By assuming the last possibility, an approximate calculation of the distribution between both pools can be made. The Stern-Volmer plot for quenching of a fluorophore distributed between two populations, 1 and 2, will follow the equation (32): $[Fo/F]_T = (f/[Fo/F]_1 + (1 - f)/[Fo/F]_2)^{-1}$, where $[Fo/F]_T$, $[Fo/F]_1$, and $[Fo/F]_2$ are the Fo/F ratios for the total fluorescence, the fluorescence of population 1, and that of population 2, respectively, and f is the fractional intensity of the fluorescence of population 1. By using the quenching data of DPH as $[Fo/F]_1$ and data of DPH-PC or DPH-prop as $[Fo/F]_2$, values of f of about 0.75 for native Lp and of about 0.55 for PL-depleted Lp, are obtained. These fractional intensities, corrected for the relative quantum yield of both pools which can be

obtained from the <τ> of DPH and DPH-PC, would correspond to molar fractions of approximately 0.7 and 0.5. As shown in Fig. 2B, the simulated curves assuming two populations are very similar to those obtained assuming a unique population, which does not allow us to distinguish between these two possibilities. However, the observed increase in τ of DPH-DAG in the presence of acrylamide (Table 2) would support the possibility of a distribution between two pools of different τ and accessibility to the quencher.

PLA_2 treatment increases accessibility to acrylamide for all the DPH-derivatives, but the largest proportional increase in quenching occurs for DPH-DAG. This fact would indicate a particularly high enhancement of acrylamide penetration in the intermediate region after PL depletion, if a localization of this probe between DPH and DPH-PC was assumed. However, the same fact would indicate that PL depletion induces a migration of the DAG analogue from the core to the surface when assuming a partition of DPH-DAG between both pools. The increased DAG/PL ratio in the surface resulting from PL depletion and this DAG redistribution could lead to the generation of packing defects in the LP surface. This would increase acrylamide penetration resulting in the enhanced quenching for the other probes besides DPH-DAG.

Tryptophan fluorescence

ApoLp-I and apoLp-II of *T. infestans* Lp contain 33 (1.6 mol%) and 3 (0.5 mol%) residues of Trp, respectively (16). The Trp fluorescence was used to investigate the possibility of a reorganization of these apoproteins, resulting from PL depletion of Lp. The Trp emission spectra, τ, and r_S of native and PLA_2-treated Lp are very similar (not shown), suggesting that PL depletion does not largely alter either the average mobility of the apoprotein Trp residues or the average polarity and rate of dipolar relaxation in the Trp environment. Also, only a small increase in the acrylamide quenching of Trp fluorescence (about 7%) was observed after PLA_2 treatment (not shown) indicating no large changes in the exposure degree of Trp residues.

To obtain information on the apoprotein Trp residue localization in Lp and their redistribution by PLA_2-treatment, energy transfer from Trp to acceptors with different localization in the Lp particle was measured. The n-AS are anchored through their carboxylate group to the interface. Thus, by increasing n, the fluorescent anthroyl moiety is located progressively at increasing depths from the interface (33). **Figure 3** shows the efficiency of energy transfer as a function of the acceptor concentration in the Lp particles for 2-, 7-, and 12-AS. In native Lp, energy transfer is minimal for 7-AS and it increases for 12-AS and specially for 2-AS. This indicates that although the major proportion of Trp residues are externally located, some of them are deeply located. PL depletion produces a decrease in energy transfer from Trp to the n-AS specially in the case of the deeply located 12-AS. For 2- and 7-AS, the maximal energy transfer reached at high acceptor concentrations is not changed by PLA_2 treatment indicating that the number of Trp residues in the proximity of these acceptors does not change. The small decrease in energy transfer observed for 2- and 7-AS at low acceptor concentrations is likely to be due to a diminished rate of the acceptor lateral diffusion, which can be produced by the increased DAG/PL ratio in the surface lipid layer. On the other hand, in the case of 12-AS, the maximal energy transfer reached at high acceptor concentration is diminished by about one third after PLA_2 treatment. The results of energy transfer from Trp to DPH and DPH-Prop are also shown in Fig. 3. PLA_2 treatment has no great effect on the energy transfer to the external acceptor DPH-Prop, but it produces an increased energy transfer to the DPH located in the hydrophobic core. These results suggest that apolipoproteins have a different conformation in PLA_2-treated and native Lp, with less Trp residues in proximity to the region where the anthroyl group of 12-AS is located and more Trp residues in the core where DPH locates.

Generalized polarization (GP) of Laurdan fluorescence

As shown in **Fig. 4,** the emission spectrum of Laurdan is blue shifted in PL-depleted Lp as compared with native Lp. Only a small decrease (about 5%) in Laurdan τ is produced by PL depletion (data not shown), indicating that the spectral shifts are the consequence of a different rate of dipole relaxation in the Laurdan environment. Laurdan locates in the interfacial region, and relaxing dipoles in this region can only be due to the water molecules present within the lipid polar groups. Thus, these results indicate that water mobility in the interfacial region is lower in PL-depleted as compared with native Lp.

A useful parameter to quantify Laurdan spectral shifts is the GP. **Figure 5** shows the excitation and emission GP as a function of the wavelength for Laurdan in native and PL-depleted Lp. The dependence of GP on the wavelength has been used to detect the coexistence of gel and liquid–crystalline phase domains in membranes (34). It must be noted that in both native and PL-depleted Lp, ex GP decreases with increasing wavelength and em GP increases with increasing wavelength, which is typical of a pure liquid crystalline phase. Thus, it indicates that at 25°C only a liquid crystalline phase is present in the surface lipid layer of both native and PLA_2-treated Lp, but water mobility in the interfacial

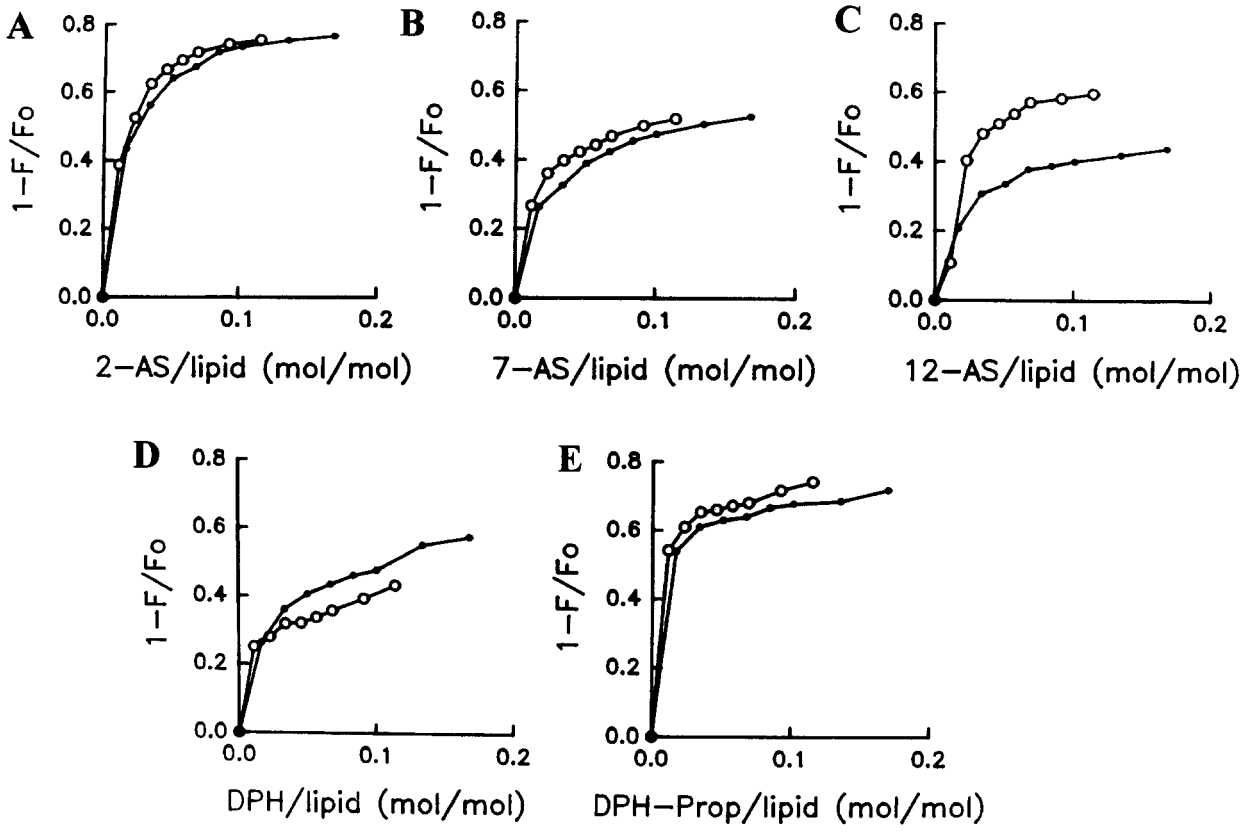

Fig. 3. Energy transfer from tryptophan to 2-AS (A), 7-AS (B), 12-AS (C), DPH (D), and Prop-DPH (E) incorporated in native (open symbols) and phospholipase A_2-treated (filled symbols) lipophorin. The energy transfer efficiency (1 - F/Fo) is plotted versus the acceptor/lipid molar ratio.

region is lower when the DAG/PL ratio in this surface layer is increased by PLA_2 treatment. By exciting the Trp residues at 290 nm and observing Laurdan fluorescence that comes from energy transfer, information on the probe molecules in the proximity to the apolipoproteins is obtained. The emission maxima of Trp occur at about 330 nm. Data in Fig. 5 show that specially for the PL-depleted Lp, GP values obtained at 290 nm excitation are significantly lower than the extrapolated values for direct excitation of Laurdan at 330 nm. This fact suggests that not only in the PLA_2-treated Lp but also to a minor degree in the native one, the water re-orientation in the interfacial region is faster in proximity to the apoproteins than in the bulk lipid region.

DISCUSSION

The localization of the lipid components in *T. infestans* Lp was studied using different DPH-derivatives. Accessibility to acrylamide and τ indicate a surface location for DPH-PC and a deep location for DPH that would report the PL and HC locations, respectively. A surface location of PL and a core location of HC in locust Lp was indicated by NMR and calorimetry (4, 7). The location of DAG is still discussed (3). From small-angle X-ray scattering studies, it has been proposed that Lp is composed of three centro-symmetrical layers (35); an outer shell with apoLp-I and PL, a middle layer with apoLp-II and DAG, and a core with HC. However, as discussed by Soulages and Wells (3), this model is not consistent with the molecular weight and radii of Lp. A composition–structure correlation (6) predicts than the majority of DAG molecules would reside in the core, with a maximum of 10 mol% in the surface. Recently, NMR studies in [^{13}C]DAG-enriched Lp of *M. sexta* (36) indicate a high degree of water exclusion from DAG carbonyls suggesting a preferential core localization, but a small fraction (less than 20%) of hydrated DAG was detected. Our results with *T. infestans* Lp suggest that the DAG analogue DPH-DAG does not belong in exactly the same lipid pool as the hydrophobic DPH. Although an intermediate localization of DAG between the core and the surface layer cannot be completely discarded, these data suggest a distribution of this probe and thus of DAG between a core pool of about 70 mol% and a

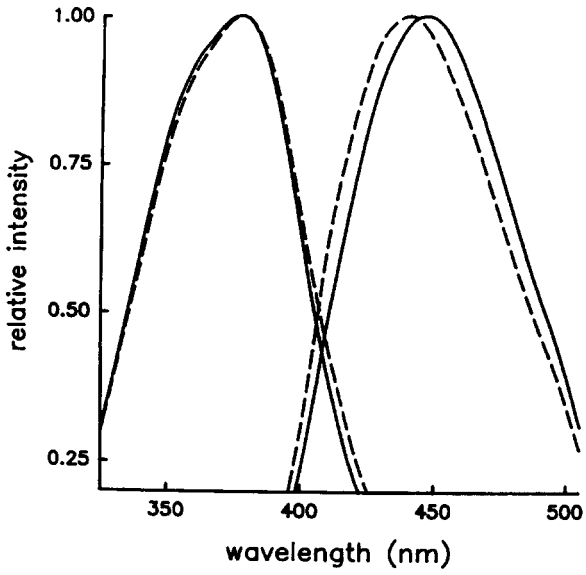

Fig. 4. Fluorescence excitation and emission spectra of Laurdan in native (- - - -) and phospholipase A_2-treated (—) lipophorin. For the excitation spectra, the emission wavelength was 480 nm, and for the emission spectra, the excitation wavelength was 360 nm.

surface pool of about 30 mol%. A higher proportion of DAG in the surface layer as compared with the above-mentioned NMR study (36) could be due to the different methodology used, but also to the higher DAG/PL ratio present in *T. infestans* Lp as compared with *M. sexta* Lp (6).

These results also indicate that PLA_2 treatment of this Lp does not change the organization of HC and PL. However, data suggest a DAG migration from the core to the surface which would compensate in a large proportion for the removal of surface PL. DAG perturbs packing in lipid membranes (37, 38), possibly due its cone-shaped molecular geometry, which would promote an increased hydration of acyl chains and concomitant bilayer destabilization. Thus, a high DAG/PL ratio in the highly curved surface layer of Lp would not be possible without stabilizing interactions with apolipoproteins. In fact, the high DAG loading in *M. sexta* Lp leads to the binding of a third apolipoprotein, apoLp-III (1, 39). ApoLp-III avoids particle aggregation in *M. sexta* Lp either after DAG enrichment (5) or after phospholipase C digestion (10). PLA_2 treatment of the apoLp-III-containing Lp of *R. prolixus* (9) and *M. sexta* (8) resulted in stable particles. As noted (3), apoLp-III could stabilize these PL-depleted particles.

However, apoLp-III was not detected in *T. infestans* Lp (16) and PLA_2 treatment resulted in stable particles. Phospholipase C treatment of HDLp wanderer 2 of *M. sexta*, which also lacks apoLp-III, also resulted in no particle aggregation. This fact was explained by proposing that DAG molecules created by PL hydrolysis partition into available space in the core (10). Our results, however, suggest that PLA_2 treatment induces a DAG output from the core to the surface of the Lp. The resulting increase in the DAG/PL ratio on the surface layer of this Lp lacking apoLp-III could only be stabilized by changes in the organization of apoLp-I and/or apoLp-II. Although no large changes in the average mobility and environment polarity of Trp were observed, a reorganization of the apoproteins was indicated by the energy transfer from Trp to 12-AS and DPH. These results suggest that after treatment with PLA_2, an appreciable proportion of apoprotein Trp located in the internal region of the surface layer sensed by 12-AS migrate to the core sensed by DPH. Thus, the free space in the core left by the DAG output would be occupied by some portions of the apoproteins. Due to the cone-shaped geometry of DAG, the decrease in the proportion of apoprotein in the internal region of the surface layer as sensed by 12-AS would help to stabilize the high DAG/PL in the surface, but an increased proportion of apoprotein would also be expected in the interfacial region. No increase in the amount of Trp near the external 2-AS probe was observed, and only a small increase in Trp accessibility to acrylamide was detected. However, the possibility that Trp-poor regions of the apoproteins can be involved in an increased lipid–protein interaction in the interfacial region is not discarded.

Increasing DAG content of *M. sexta* Lp decreased the DPH r_S (5). Our results indicate that PLA_2 treatment produces a small increase in the DPH r_S that was the result of a moderate decrease in the amplitude of wob-

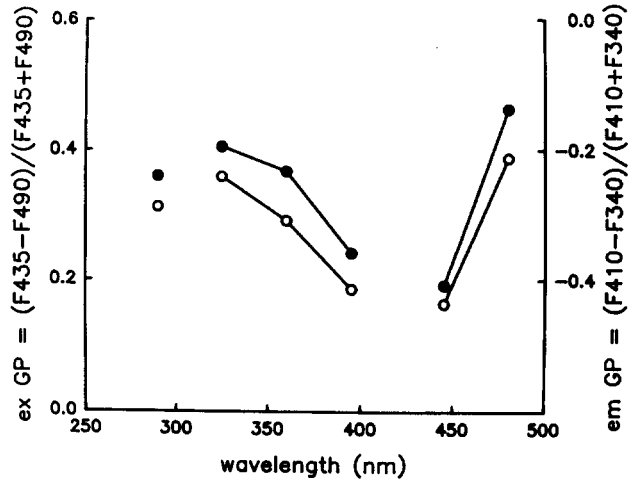

Fig. 5. Generalized polarization excitation (ex GP) and emission (em GP) spectra of Laurdan in native (open symbols) and phospholipase A_2-treated (filled symbols) lipophorin. The values of Laurdan ex GP that result from energy transfer from tryptophan by exciting at 290 nm are also included.

bling. This change in the DPH rotational behavior may be due to the decreased lipid/protein ratio or DAG content that is produced in the Lp core after PLA_2 treatment. The high DPH r_S values in Lp of *T. infestans* would be due to the lipid motional restriction imposed by the apolipoproteins, as lower r_S values were found in dispersions of the extracted lipids (6). Comparatively lower DPH r_S values were reported for *M. sexta* Lp (5). The high r_S values are principally due to a high degree of hindering to the DPH wobbling as indicated by the high r_∞ obtained. An even larger hindering to the wobbling amplitude was found for the probes localized in the surface layer.

These results also showed that PLA_2 treatment affected the Lp interfacial properties. Some increase in acrylamide penetration was observed which could be ascribed to packing defects produced by the high DAG/PL ratio in the surface layer. These effects seem to be localized just in the external region of the surface layer as reported by the τ increase for DPH-TMA in comparison with other probes with deeper localization in this layer such as DPH-Prop and DPH-PC. A decrease in the wobbling amplitude of DPH-TMA and a diminished mobility of the water in the interfacial region by Laurdan were also produced after PL depletion. In PC/DAC sonicated liposomes, Laurdan GP increased as the DAG content increased from 0 to 10% (w/w), although very much lower GP values were obtained in these liposomes as compared with those reported here for Lp (O. J. Rimoldi and H. A. Garda, personal communication). This fact indicates that the effect of PLA_2 treatment on Laurdan GP in Lp could be a direct consequence of increased DAG/PL ratio in the surface layer, but also because of the increased protein to lipid ratio. The reduced motion in the interfacial region produced by PL depletion could also diminish the lipid lateral mobility as it is suggested by the results of energy transfer from Trp to 2- and 7-AS. This is in accordance with ^{31}P-NMR studies that indicated a slower PL lateral diffusion in the DAG-rich LDLp in comparison with other DAG-poor Lp of *M. sexta* (40).

DPH and parinaric acids sense lipid thermotropic transitions in *T. infestans* Lp at about 20°C, and in Lp lipid dispersions at about 30°C (6). Thus, the decreased lipid mobility in the surface layer observed after PLA_2 treatment could be due to gel phase formation. However, the wavelength dependence of Laurdan GP indicates the absence of gel phase at 25°C.

In short, this report shows that PL depletion of *T. infestans* Lp by PLA_2 treatment results in stable particles with an increased DAG/PL ratio in the surface layer. The modified Lp particles are possibly stabilized by a change in the conformation of the apolipoproteins.

This work was supported by a grant from the Consejo Nacional de Investigaciones Cientíificas y Técnicas (CONICET), Argentina, and by Efamol Research Inc., Canada. The authors are members of the Carrera del Investigador Científico, CONICET, Argentina.

Manuscript received 15 April 1996 and in revised form 1 July 1996.

REFERENCES

1. Beenakkers, A. M., A. M. T. Van der Horst, and W. J. A. Van Marrewijk. 1985. Insect lipids and lipoproteins and their role in physiological processes. *Prog. Lipid Res.* **24:** 19–67.
2. Law, J. H., and M. A. Wells. 1989. Insects as biochemical models. *J. Biol. Chem.* **264:** 16335–16338.
3. Soulages, J. L., and M. A. Wells. 1994. Lipophorin: the structure of an insect lipoprotein and its role in lipid transport in insect. *Adv. Protein Chem.* **45:** 371–415.
4. Katagiri, C., J. Kimura, and N. Murase. 1985. Structural studies of lipophorin in insect blood by differential scanning colorimetry and ^{13}C-nuclear magnetic relaxation measurements: location of hydrocarbons. *J. Biol. Chem.* **260:** 13490–13495.
5. Soulages, J. L., and M. A. Wells. 1994. Effect of diacylglycerol content on some physicochemical properties of the insect lipoprotein, lipophorin. Correlation with the binding of apolipophorin-III. *Biochemistry.* **33:** 2356–2362.
6. Soulages, J. L., and R. R. Brenner. 1990. Study of composition–structure relationship of lipophorins. *J. Lipid Res.* **32:** 407–415.
7. Katagiri, C. 1985. Structure of lipophorin in insect blood: location of phospholipid. *Biochim. Biophys. Acta.* **834:** 139–143.
8. Kawooya, J. K., D. J. van der Horst, B. L. J. van Heusden, J. Brigot, R. van Antwerpen, and J. H. Law. 1991. Lipophorin structure analized by in vitro treatment with lipases. *J. Lipid Res.* **32:** 1781–1788.
9. Gondin, K. C., G. C. Atella, J. K. Kawooya, and H. Masuda. 1992. Role of phospholipids in the lipophorin particles of Rhodnius prolixus. *Arch. Insect Biochem. Physiol.* **20:** 303–314.
10. Amareshwar Singh, T. K., H. Liu, R. Bradley, D. Scraba, and R. O. Ryan. 1994. Effect of phospholipase C and apolipophorin III on the structure and stability of lipophorin subspecies. *J. Lipid Res.* **35:** 1561–1569.
11. Lakowicz, J. R. 1983. Principles of Fluorescence Spectroscopy. J. R. Lakowicz, editor. Plenum Press, New York, NY. 171–178.
12. Lakowicz, J. R., F. G. Prendergast, and D. Hogen. 1979. Differential polarized phase fluorometric investigations of diphenylhexatriene in lipid bilayers. Quantitation of hindered depolarizing rotations. *Biochemistry.* **18:** 508–519.
13. Chalpin, D. B., and A. M. Kleinfeld. 1983. Interaction of fluorescent quenchers with the n-(9-anthroyloxy) fatty acid membrane probes. *Biochim. Biophys. Acta.* **731:** 465–474.
14. Parasassi, T., G. De Stasio, A. d'Ubaldo, and E. Gratton. 1990. Phase fluctuation in phospholipid membranes revealed by Laurdan fluorescence. *Biophys. J.* **57:** 1179–1186.
15. Parasassi, T., G. De Stasio, G. Ravagnan, R. M. Rusch, and E. Gratton. 1991. Quantitation of lipid phases in phos-

pholipid vesicles by the generalized polarization of Laurdan fluorescence. *Biophys. J.* **60:** 179–189.
16. Rimoldi, O. J., J. L. Soulages, M. S. González, R. O. Peluffo, and R. R. Brenner. 1990. Biochemistry of the evolution of *Triatoma infestans*. XI. Hemolymph lipophorin. *Acta Physiol. Pharmacol. Latinoam.* **40:** 239–255.
17. Lowry, O. H., N. J. Rosebrough, A. L. Farr, and R. J. Randall. 1951. Protein measurement with the Folin phenol reagent. *J. Biol. Chem.* **193:** 265–275.
18. Ornstein, L., and B. J. Davis. 1964. Disc electrophoresis I and II. *Ann. N.Y. Acad. Sci.* **121:** 321–349, 404–427.
19. Folch, J., M. Lees, and G. H. Sloane Stanley. 1957. A simple method for isolation and purification of total lipids from animal tissues. *J. Biol. Chem.* **226:** 497–509.
20. Lakowicz, J. R., and H. Cherek. 1980. Dipolar relaxation in proteins on the nanosecond timescale observed by wavelength-resolved phase fluorometry of tryptophan fluorescence. *J. Biol. Chem.* **255:** 831–834.
21. Spencer, R. D., and G. Weber. 1970. Influence of brownian rotations and energy transfer upon the measurements of fluorescence lifetime. *J. Chem. Phys.* **52:** 1654–1663.
22. Lakowicz, J. R., H. Cherek, and D. R. Bevan. 1980. Demonstration of nanosecond dipolar relaxation in biopolymers by inversion of apparent fluorescence phase shift and demodulation lifetimes. *J. Biol. Chem.* **255:** 4403–4406.
23. Prendergast, F. G., R. P. Haugland, and P. J. Callahan. 1981. 1-[4-(Trimethylamino)phenyl]-6-phenylhexa-1,3,5-triene synthesis, fluorescent properties and use as a fluorescent probe of lipid bilayers. *Biochemistry.* **20:** 7333–7338.
24. Lakowicz, J. R., H. Cherek, and A. Balter. 1981. Correction of timing errors in photomultiplier tubes used in phase-modulation fluorometry. *J. Biochem. Biophys. Methods.* **5:** 131–146.
25. Weber, G. 1978. Limited rotational motion: recognition by differential phase fluorometry. *Acta Physiol. Pol.* **A54:** 173–179.
26. Tricerri, M. A., H. A. Garda, and R. R. Brenner. 1994. Lipid chain order and dynamics at different bilayer depths in liposomes of several phosphatidylcholines studied by differential polarized phase fluorescence. *Chem. Phys. Lipids.* **71:** 61–72.
27. Garda, H. A., A. M. Bernasconi, and R. R. Brenner. 1994. Possible compensation of structural and viscotropic properties in hepatic microsomes and erythrocyte membranes of rats with essential fatty acid deficiency. *J. Lipid Res.* **35:** 1367–1377.
28. Garda, H. A., A. M. Bernasconi, and R. R. Brenner. 1994. Influence membrane proteins on lipid matrix structure and dynamics. A differential polarized phase fluorometry study in rat liver microsomes and erythrocyte membranes. *Anal. Asoc. Quím. Arg.* **82:** 305–323.
29. Parasassi, T., M. Loiero, M. Raimondi, G. Ravagnan, and E. Gratton. 1993. Absence of lipid gel-phase domains in seven mammalian cell lines and in four primary cell types. *Biochim. Biophys. Acta.* **1153:** 143–154.
30. Fiorini, R., M. Valentino, S. Wang, M. Glaser, and E. Gratton. 1987. Fluorescence lifetime distribution of 1,6-diphenyl-1,3,5-hexatriene in phospholipid vesicles. *Biochemistry.* **26:** 3864–3870.
31. Kutchai, H., L. H. Chandler, and G. B. Zavoico. 1983. Effects of cholesterol on acyl chain dynamics in multilamellar vesicles of various phosphatidylcholines. *Biochim. Biophys. Acta.* **736:** 137–149.
32. Eftink, M. R., and C. A. Ghiron. 1981. Fluorescence quenching studies with proteins. *Anal. Biochem.* **114:** 199–227.
33. Abrams, F. S., A. Chattopadhyay, and E. London. 1992. Determination of the location of fluorescent probes attached to fatty acids using parallax analysis of fluorescent quenching: effect of carboxyl ionization state and environment on depth. *Biochemistry.* **31:** 5322–5327.
34. Parasassi, T., G. Ravagnan, R. H. Rusch, and E. Gratton. 1993. Modulation and dynamics of phase properties in phospholipid mixtures detected by Laurdan fluorescence. *Photochem. Photobiol.* **57:** 403–410.
35. Katagiri, C., M. Sato, and N. Tanaka. 1987. Small-angle X-ray scattering study of insect lipophorin. *J. Biol. Chem.* **262:** 15857–15861.
36. Soulages, J. L., M. Rivera, A. Walker, and M. A. Wells. 1994. Hydration and localization of diacylglycerol in the insect lipoprotein lipophorin. A ^{13}C-NMR study. *Biochemistry.* **33:** 3245–3251.
37. Siegel, D. P., J. Banschbach, D. Alford, H. Ellens, L. Lis, P. J. Quinn, P. L. Yeagle, and J. Bentz. 1989. Physiological levels of diacylglycerols in phospholipid membranes induce membrane fusion and stabilize inverted phases. *Biochemistry.* **28:** 3703–3709.
38. De Boeck, H., and R. Zidovetzki. 1989. Effect of diacylglycerols on the structure of phosphatidyl-choline bilayers: a ^{2}H and ^{31}P NMR study. *Biochemistry.* **28:** 7439–7446.
39. Wells, M. A., R. O. Ryan, J. K. Kawooya, and J. H. Law. 1987. The role of apolipophorin III in in vivo lipoprotein interconversion in adult *Manduca sexta*. *J. Biol. Chem.* **262:** 4172–4176.
40. Wang, J., H. Liu, B. D. Sykes, and R. O. Ryan. 1992. ^{31}P-NMR study of the phospholipid moiety of lipophorin of subspecies. *Biochemistry.* **31:** 8706–8712.